Desalination and Water Treatment
www.deswater.com

doi: 10.5004/dwt.2017.21182

81 (2017) 199–208
June

Evaluation of Fenton and photo-Fenton processes for the removal of *p*-chloronitrobenzene in aqueous environment using Box–Behnken design method

Majid Mohadesi[a], Aref Shokri[b,*]

[a]*Department of Chemical Engineering, Faculty of Energy, Kermanshah University of Technology, Kermanshah, Iran, email: m.mohadesi@kut.ac.ir*
[b]*Young Researchers and Elite Club, Arak Branch, Islamic Azad University, Arak, Iran, email: aref.shokri3@gmail.com*

Received 17 February 2017; Accepted 6 July 2017

ABSTRACT

In this study, the degradation and mineralization of aqueous solution containing a main carcinogenic pollutant, *p*-chloronitrobenzene (pCNB), were investigated by Fenton and photo-Fenton processes. Also the influence of operational parameters such as initial concentrations of H_2O_2, ferrous ion and pCNB has been studied on the removal of pCNB and chemical oxygen demand (COD). The pH was fixed at 3.00 in all experiments. The Box–Behnken design (BBD) of experiments and the response surface methodology were used to explore the influences of three independent variables on the response functions to get the optimal conditions. The analysis of variance tests were performed to determine the significance of the effects of independent variables on the response function. Different amounts of variables were optimized for the removal of pCNB and COD in both Fenton and photo-Fenton processes. At optimum conditions and after 20 min of reaction, the removal efficiency for pCNB was 98.5% and 100.0% in Fenton and photo-Fenton processes, respectively. The removal of COD in photo-Fenton process was more effective (91.4%) than Fenton process (58.5%) after 30 min of treatment. The Fenton process was powerful in the removal of pCNB, but it can remove the COD to some extent.

Keywords: Fenton and photo-Fenton processes; *p*-Chloronitrobenzene; Box–Behnken design; Chemical oxygen demand; Wastewater treatment

1. Introduction

A typical halogenated nitro aromatic compound that is extensively used in the production of herbicides, pesticides, antioxidants and other industrial chemicals is *p*-chloronitrobenzene (pCNB). It has been specified that pCNB can hold mutagenic and carcinogenic characteristics and cause methemoglobinemia in humans and animals. Thus, the elimination of this pollutant from aqueous environment is significant for the environment and human health [1]. There are few studies in the literature about pCNB degradation. Shen et al. [2] have investigated degradation of pCNB in water by ozonation. Liu et al. [3] studied the removal of pCNB by manganese silicate catalyzed ozonation and so on. There are three classical techniques for the remediation of industrial wastewater, including: physical, chemical and biological methods. The classical methods have great operational costs, secondary pollution and long reaction time, so employing new methods without these difficulties is needed. Advanced oxidation processes (AOPs) produce powerful oxidant species such as hydroxyl radicals that can be broadly used for the removal of organic pollutants which are difficult to eliminate by biological treatment ways.

Various AOPs have been employed for degradation of aromatic pollutants in aqueous phase. For example, heterogeneous photocatalysis such as TiO_2, ozonation [4–7], UV/H_2O_2 [8], Fenton and photo-Fenton processes [9–11] have been used for this purpose. The Fenton and photo-Fenton methods are a good choice because they need minor energy and low cost of chemicals (ferrous salt and hydrogen peroxide) [12,13].

* Corresponding author.

The manuscript was written through contribution from all authors. All authors have given approval to the final version of the manuscript.

It is clear that the Fenton technique generates hydroxyl radicals ($HO^{\bullet}$) efficiently as a result of the reaction between Fe(II) and H_2O_2:

$$H_2O_2 + Fe^{2+} \rightarrow OH^{\bullet} + OH^{-} + Fe^{3+} \quad (1)$$

$$H_2O_2 + Fe^{3+} \rightarrow HOO^{\bullet} + H^{+} + Fe^{2+} \quad (2)$$

Furthermore, Fe(III) can interact with the leftover hydrogen peroxide, giving back Fe(II) (Eq. (2)) [14]. In the photo-Fenton process, the photo-reduction of ferric to ferrous ions is improved with the production of additional $OH^{\bullet}$ radicals, so the oxidation of pollutants was increased.

The main objective of this study is to use a Box–Behnken design (BBD) method for the optimization of operational parameters on degradation and mineralization of pCNB in Fenton and photo-Fenton processes.

2. Materials and methods

2.1. Materials

pCNB (99.5% purity) was purchased from Merck company of Germany and used without further purification. Ferrous sulphate heptahydrate ($FeSO_4$ $7H_2O$) as the source of Fe(II), hydrogen peroxide solution (30% w/w), H_2SO_4 and NaOH are all supplied from Merck. Distilled water was used in all of the experiments.

2.2. Experimental set-up

In this project, experiments were performed in a glass cylindrical batch photoreactor with 1 L capacity. The system was equipped with a sampling system (Fig. 1). The light source was a mercury lamp, Philips 15 W (UV-C), which was immersed vertically in the center of the reactor. The reactor was equipped with a jacket of water and external circulating flow through a thermostat for regulating temperature fixed at 25°C. The solution in the reactor was mixed well by a stirrer. A pH meter, PT-10P Sartorius Instrument from German company, was employed to regulate the initial pH of the solution. Water bath, BW 20G model from Korean company, was used for fixing temperature at 25°C in all experiments. The advancement in the degradation of pCNB was calculated with high-performance liquid chromatography (HPLC) from Knauer, Germany, and it was equipped with spectrophotometer (platinum blue, Germany). A reverse phase column with 150 mm in length and 4.6 mm in diameter was filled with 3 μm Separon C_{18}. The isocratic method was employed with a solvent mixture of 30% deionized water and 70% of methanol with a flow rate of 1 mL min^{-1}. The volume of injected sample was 10 μL and the detection wavelength was 260 nm. Using the spectrophotometer (DR 5000, Hach, Jenway, USA), the absorbance of chemical oxygen demand (COD) samples was estimated with a wavelength of 600 nm.

2.3. General procedure

Exactly 1,000 mL of synthesized wastewater containing pCNB was used during each experiment. Different concentrations of pCNB, H_2O_2 and Fe^{2+} were used for optimization

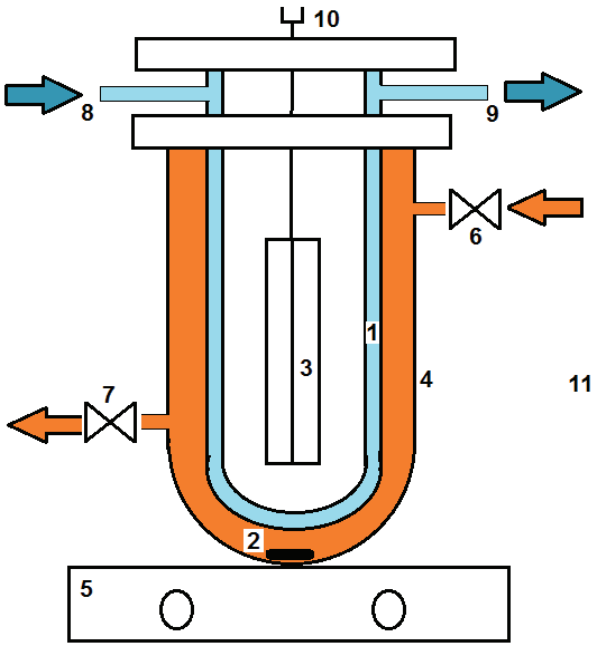

Fig. 1. Schematic diagram of the used reactor in laboratory scale. (1) Quartz immersion well, (2) magnetic stirrer bar, (3) UV lamp, (4) glass reactor, (5) magnetic stirrer, (6) loading valve, (7) unloading valve and sampling point, (8) cooling water supply, (9) cooling water return, (10) electric connection and (11) dark box.

in Fenton and photo-Fenton processes. An aqueous solution containing 10% of sodium sulphite was employed to quench the reactions. In the photo-Fenton process, the UV lamp was switched on to start the reaction. The solution was mixed by a stirrer to prevent the settling of iron ions in the reactor and preserves the suspension to be homogenous. The samples were withdrawn and determined by UV/Vis spectrophotometer and validated by HPLC. COD was measured based on standard methods [15]. The suitable efficiencies were calculated with respect to its initial values and the removal percentage for the pCNB and COD were gained as in Eqs. (3) and (4):

$$\text{Removal of pCNB}\,(\%) = \left(\frac{[\text{pCNB}]_0 - [\text{pCNB}]}{[\text{pCNB}]_0}\right) \times 100 \quad (3)$$

$$\text{Removal of COD}\,(\%) = \left(\frac{[\text{COD}]_0 - [\text{COD}]}{[\text{COD}]_0}\right) \times 100 \quad (4)$$

where $[pCNB]_0$ and $[COD]_0$ are the concentration of the pCNB and amount of COD at the start of the reaction and [pCNB] and [COD] are the concentration of the pCNB and amount of COD at time *t*, respectively.

The residual amount of hydrogen peroxide in the samples had interference with COD test and it was removed by MnO_2 powder. Samples were filtered for separation of MnO_2 powders [16].

2.4. Experimental design

The experimental design method was used and the percentage of the degradation and mineralization

of the pCNB was selected as responses to consider the optimum conditions. The process depends on different variables comprising the concentration of H_2O_2, Fe^{2+} and pCNB in Fenton and photo-Fenton processes. The BBD was employed with three independent variables involving the concentration of ferrous ion (C_F), hydrogen peroxide (C_{HP}) and pCNB (C_{pCNB}). The pH was fixed at 3.00 in all experiments based on the preliminary tests. The input variables and their levels in the experiment were presented in Table 1.

2.5. Data analysis

Among all other response surface methodology (RSM) designs, Box–Behnken experimental designs need less runs (15 runs for three variables) [17]. According to the experimental design, the following model was fitted to the response variable (Y) in the form of a polynomial equation (Eq. (5)):

$$Y = b_0 + \sum b_i x_i + \sum\sum b_{ij} x_i x_j + \sum\sum b_{ii} x_i^2 + \varepsilon \quad (5)$$

where b_0 is a constant; ε is the residual term; b_{ij} is the linear interaction effect between the input variables, x_i and x_j (i = 1, 2 and 3; j = 1, 2 and 3); b_i is the slope of the variable; b_{ii} is the second order of input variable (x_i). The analysis of variance (ANOVA) was used to explore the significance of each term in the polynomial equation [18]. The Minitab 17 was employed to determine the coefficients of Eq. (5) by RSM. The experimental design included 15 tests and the natural values of these factors for the removal of pCNB are shown in Table 2. All experiments were performed accidentally to minimize the experimental errors. Two responses, removal efficiencies of pCNB and COD, were obtained from experiments mentioned in Table 2.

Table 1
The range and level of the variables

Factors	Symbol	Range and levels		
		–1	0	+1
Ferrous, mM	C_F	0.08	0.14	0.20
Hydrogen peroxide, mM	C_{HP}	2.0	4.0	6.0
p-Chloronitrobenzene, mM	C_{pCNB}	0.21	0.42	0.63

3. Results and discussion

3.1. Central composite design model

The main purpose of this section was to determine the optimum condition for maximum removal of pCNB and COD in Fenton and photo-Fenton processes. The stages of central composite design (CCD) were investigated by many researchers [19,20]. The two responses, three-factors CCD matrix and experimental results achieved by the removal of the pCNB and COD are presented in Table 2.

The correctness of the model are exemplified in Fig. 2, which compares the experimental values vs. the predicted responses of the model for the degradation of pCNB.

3.2. ANOVA tests for the removal of pCNB by Fenton and photo-Fenton processes

In this study, by using the BBD and the RSM, the influences of three independent variables on the response functions were explored to get the optimal conditions. The mathematical relation between the responses and three important variables can be estimated by a quadratic polynomial equation [21]. The equations for the removal of the pCNB in Fenton and photo-Fenton processes are presented in the following equations:

Table 2
Experimental design for three independent variables and the responses

Run no.	Manipulated variables			Responses, %			
	X_{C_F}	$X_{C_{HP}}$	$X_{C_{pCNB}}$	$pCNB_F$	$pCNB_{PF}$	COD_F	COD_{PF}
1	–1	0	+1	46.5	78.0	24.5	49.0
2	+1	0	+1	52.0	71.5	30.0	42.5
3	–1	+1	0	71.5	94.0	40.0	64.0
4	–1	–1	0	60.0	86.0	37.0	59.0
5	–1	0	–1	94.0	100.0	56.0	89.0
6	+1	0	–1	98.5	99.0	58.5	79.5
7	0	–1	+1	31.0	49.0	7.3	30.7
8	+1	–1	0	67.0	82.3	39.0	53.0
9	0	0	0	76.5	96.0	42.0	75.0
10	0	+1	–1	97.0	100.0	57.0	86.0
11	0	–1	–1	91.5	98.0	53.5	79.0
12	+1	+1	0	72.5	89.0	39.5	57.0
13	0	+1	+1	49.0	70.0	28.7	40.5
14	0	0	0	76.0	95.0	42.0	74.0
15	0	0	0	76.0	97.0	41.0	74.6

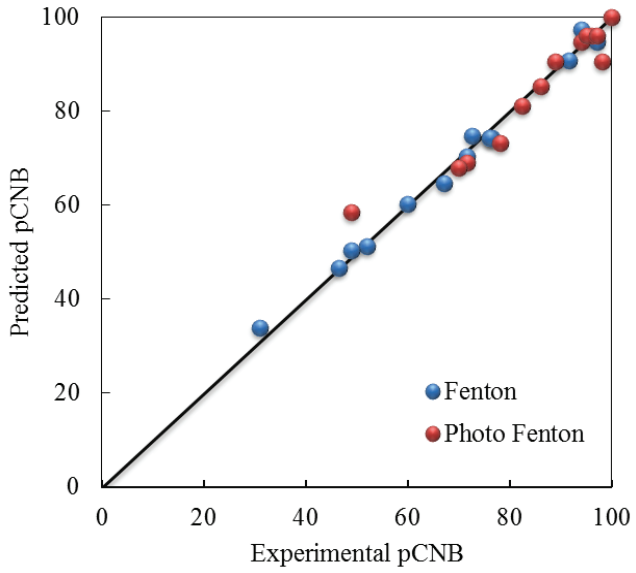

Fig. 2. Comparing the experimental and predicted values for the removal of pCNB in Fenton and photo-Fenton processes.

$$pCNB_F = 74.21 + 2.25X_{C_F} + 5.06X_{C_{HP}} - 25.31X_{C_{pCNB}} + 3.12X_{C_{HP}}X_{C_{pCNB}} - 6.78X^2_{C_{HP}} \quad (6)$$

$$pCNB_{PF} = 95.91 - 2.03X_{C_F} + 4.71X_{C_{HP}} - 16.06X_{C_{pCNB}} - 8.01X^2_{C_{HP}} - 8.71X^2_{C_{pCNB}} \quad (7)$$

In all 15 runs, the experiments were conducted in duplicated and all achieved results from the BBD are presented in Table 3. The observed values and predicted response values with residuals for all runs are presented in Table 3.

Different dosages of Fe^{2+} (from 0.08 to 0.20 mM) were used to reach its optimum concentration. As it can be seen from Fig. 3, in Fenton process the removal efficiency of pCNB was increased by an increase in the dosage of ferrous ion according to the following equations:

$$H_2O_2 + Fe^{2+} \rightarrow OH^{\bullet} + OH^- + Fe^{3+} \quad (8)$$

$$OH^{\bullet} + Fe^{2+} \rightarrow OH^- + Fe^{3+} \quad (9)$$

In Fenton process, the production of hydroxyl radicals and subsequently the removal of pCNB were enhanced by

Table 3
ANOVA tests for quadratic models in the removal of pCNB by Fenton and photo-Fenton processes

Sources	SS	DF	MS	*F*-value	*p* value
Fenton					
Model	5,581.83	5	1,116.37	161.34	<0.0001
X_{C_F}	40.50	1	40.50	5.85	0.0387
$X_{C_{HP}}$	205.03	1	205.03	29.63	0.0004
$X_{C_{pCNB}}$	5,125.78	1	5,125.78	740.81	<0.0001
$X_{C_{HP}}X_{C_{pCNB}}$	39.06	1	39.06	5.65	
$X^2_{C_{pCNB}}$	171.45	1	171.45	24.78	
Residual error	62.27	9	6.92		
Lack of fit	62.11	7	8.87	106.47	0.0093
Pure error	0.17	2	0.083		
Total	5,644.10	14			
Photo-Fenton					
Model	2,760.45	5	552.09	22.80	<0.0001
X_{C_F}	32.81	1	32.81	1.36	0.2743
$X_{C_{HP}}$	177.66	1	177.66	7.34	0.0240
$X_{C_{pCNB}}$	2,064.03	1	2,064.03	85.26	<0.0001
$X^2_{C_{HP}}$	238.51	1	238.51	9.85	0.0120
$X^2_{C_{pCNB}}$	282.00	1	282.00	11.65	0.0072
Residual error	217.89	9	24.21		
Lack of fit	215.89	7	30.84	30.84	0.0318
Pure error	2.00	2	1.00		
Total	2,978.34	14			

an increase in the concentration of Fe^{2+} ions from 0.08 to 0.20 mM. But in the photo-Fenton ones, the removal efficiency of pCNB was decreased by an increase in the dosage of ferrous ion from 0.08 to 0.20 mM after 20 min of reaction (Fig. 4). The reason is that at high concentration of Fe(II), the initial generation rate of hydroxyl radicals, mostly formed from the breakdown of H_2O_2, was so high that many of the hydroxyl radicals were spent by the side

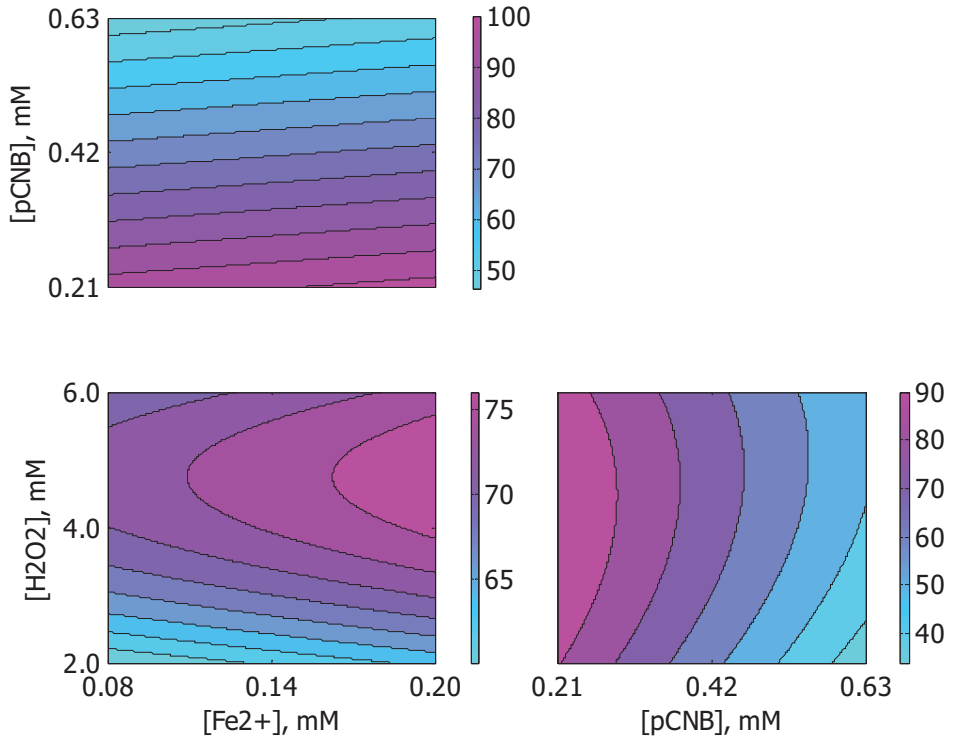

Fig. 3. The contour plot for the removal of pCNB in Fenton process based on $[Fe^{2+}]$, $[H_2O_2]$ and [pCNB].

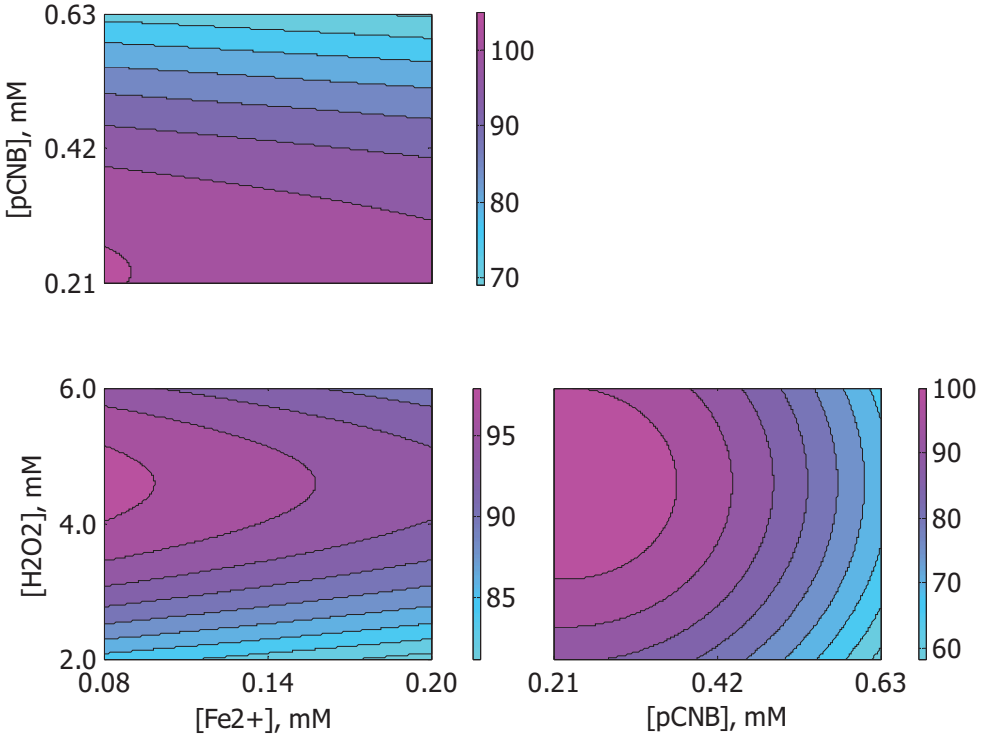

Fig. 4. The contour plot for the removal of pCNB in photo-Fenton process based on $[Fe^{2+}]$, $[H_2O_2]$ and [pCNB].

reactions before they could be consumed effectively for the removal of the pCNB [22]:

$$H_2O_2 + hv \rightarrow 2OH^{\bullet} \quad (10)$$

Additionally, high dosages of ferrous ion can lead to the brown turbidity of the solution, so the absorption of the UV light that is essential for photolysis was delayed and the recombination of $OH^{\bullet}$ radicals occurred. This result is in coincidence with the findings of many investigators [23,24].

$$FeOH^{2+} + hv \rightarrow Fe^{2+} + OH^{\bullet} \quad (11)$$

3.3. Effect of initial concentration of hydrogen peroxide

The effect of initial dosage of hydrogen peroxide on the removal efficiency of pCNB is presented in Figs. 3 and 4 for Fenton and photo-Fenton, respectively. The removal of pCNB was improved by an increase in the concentration of H_2O_2 from 2.0 to 4.0 mM, because more $OH^{\bullet}$ radicals were created and degradation efficiency was enhanced. But, by increasing in the dosages from 4.0 to 6.0 mM, the advancement was not significant or even it was falling. The hydrogen peroxide acts as free-radical scavenger at high concentrations, so the degradation efficiency was not considerable [25]. Furthermore, this trend may be based on the autodecomposition of H_2O_2 to oxygen and water and the reaction of H_2O_2 with hydroxyl radicals instead of pCNB molecules. This concept is in agreement with the findings of Oancea and Meltzer [26].

The optimum dosage of H_2O_2 was 4.7 and 4.6 mM for the removal of pCNB in Fenton and photo-Fenton processes, respectively. Thus, H_2O_2 should be added at an optimum dosage to get the best results. However, all of the added hydrogen peroxide was not spent. One of the main benefits of the photo-Fenton process against Fenton ones is low remaining of H_2O_2 in the solution.

Optimum values for maximization of pCNB removal by Fenton and photo-Fenton processes were obtained using Eqs. (6) and (7) and Figs. 3 and 4. The maximum values for the removal of pCNB through Fenton process ($pCNB_F$) is at [pCNB] = 0.21, $[Fe^{2+}]$ = 0.20 and $[H_2O_2]$ = 4.7. The value of $pCNB_F$ by model (Eq. 6) and experiment is 101.6 and 98.5, respectively. Also the maximum values for the removal of pCNB through photo-Fenton process ($pCNB_{PF}$) is at [pCNB] = 0.21, $[Fe^{2+}]$ = 0.08 and $[H_2O_2]$ = 4.6. The value of $pCNB_{PF}$. obtained by model (Eq. 7) and experiment is 106.0% and 100.0%, respectively. So the relative errors of $pCNB_F$ and $pCNB_{PF}$ models (in optimum point) are 3.14% and 6.00%, respectively.

3.4. ANOVA test for quadratic models in the removal of COD

The objective of this section was to achieve the optimal conditions for maximum removal of COD by Fenton (COD_F) and photo-Fenton (COD_{PF}) processes. The BBD can offer an empirical relationship between the response function and the variables. The mathematical relationship between the removal of COD and the three important variables can be approached by quadratic polynomial equation, as it was presented in the following:

$$COD_F = 39.73 + 1.19X_{C_F} + 3.55X_{C_{HP}} - 16.81X_{C_{pCNB}} + 4.48X_{C_{HP}}X_{C_{pCNB}} \quad (12)$$

$$COD_{PF} = 74.53 - 3.63X_{C_F} + 3.23X_{C_{HP}} - 21.35X_{C_{pCNB}} - 5.17X^2_{C_F} - 11.12X^2_{C_{HP}} - 4.37X^2_{C_{pCNB}} \quad (13)$$

The equations are used to calculate the removal of COD at each concentration of pCNB, Fe^{2+} and H_2O_2. According to the coefficients of Eqs. (12) and (13), it is obvious that the variable that had more effect was the concentration of pollutant (pCNB) with the largest coefficient and it had a negative influence on COD removal efficiency. The removal of COD was reduced by increasing the concentration of pCNB while it was enhanced with increasing the dosages of Fe^{2+} and H_2O_2. In the photo-Fenton process, the dosage of Fe^{2+} had more effect than H_2O_2 on the removal efficiency of COD. The ANOVA tests were performed in the removal of COD to determine the significance of independent variables on the response function [27]. The statistical properties of the model terms for explaining the removal efficiency of COD as a function of the studied variables are presented in Table 4.

According to the analysis, it was clear that the model terms with a probability value larger than 0.05 are not significant. It is clear that the effect of ferrous ion concentration was not significant (p = 0.4361) [28]. The significance of the coefficients is presented in Table 4.

Using Eqs. (12) and (13) and Figs. 6 and 7, optimum values of operating parameters are determined to maximize the removal of COD in Fenton and photo-Fenton processes. These values are [pCNB] = 0.21, $[Fe^{2+}]$ = 0.20 and $[H_2O_2]$ = 4 for Fenton process and [pCNB] = 0.21, $[Fe^{2+}]$ = 0.12 and $[H_2O_2]$ = 4.3 for photo-Fenton process. In these values, COD_F and COD_{PF} using models (Eqs. (12) and (13)) are 57.7% and 92.4%, respectively. These values by experiment are obtained as 58.5% and 91.4%, respectively. The relative errors for COD_F and COD_{PF} models in optimum point are 1.37% and 1.09%, respectively.

These results revealed a good agreement between predicted and experimental values for the removal of pCNB and COD in Fenton and photo-Fenton process. It was found that the predicted responses from the model are in agreement with the experimental values. This can be further illustrated by plotting the predicted values vs. the experimental data.

Diagnostic plots such as the predicted vs. actual values were used for judging the model suitability. The main diagnostic plots are employed to determine the residual analysis of the response surface design, confirming that the statistical assumptions fit the analysis data [29]. Fig. 5 exhibits a good convergence between the simulated and experimental values of the COD removal efficiency. The accuracy of the model is explained in Fig. 5, which compares the measured values against the predicted responses of the model for the removal of COD.

In the wastewater remediation process, the intermediate products of some organic pollutants can occasionally be more noxious than the initial compound. The total concentration of organics in the solution has been introduced as COD values and it is important to measure the COD after the degradation of the pollutants to verify the mineralization amount of the pCNB. Therefore, in this study the reduction of COD

Table 4
ANOVA tests for quadratic models for the removal of COD in Fenton and photo-Fenton processes

Sources	SS	DF	MS	*F*-value	*p* value
Fenton					
Model	2,453.49	4	613.37	35.78	<0.0001
X_{C_F}	11.28	1	11.28	0.66	0.4361
$X_{C_{PH}}$	100.82	1	100.82	5.88	0.0357
$X_{C_{pCNB}}$	2,261.28	1	2,261.28	131.91	<0.0001
$X_{C_{PH}} X_{C_{pCNB}}$	80.10	1	80.10	0.056	0.0560
Residual error	171.43	10	17.14		
Lack of fit	170.76	8	21.35	64.04	0.0155
Pure error	0.67	2	0.33		
Total	2,624.91	14			
Photo-Fenton					
Model	4,398.57	6	733.09	119.75	<0.0001
X_{C_F}	105.13	1	105.13	17.17	0.0032
$X_{C_{PH}}$	83.20	1	83.20	13.59	0.0062
$X_{C_{pCNB}}$	3,646.58	1	3,646.58	595.64	<0.0001
$X^2_{C_F}$	98.56	1	98.56	16.10	0.0039
$X^2_{C_{HP}}$	456.30	1	456.30	74.53	<0.0001
$X^2_{C_{pCNB}}$	70.40	1	70.40	11.50	0.0095
Residual error	48.98	8	6.12		
Lack of fit	48.47	6	8.08	31.89	0.0307
Pure error	0.51	2	0.25		
Total	4,447.54	14			

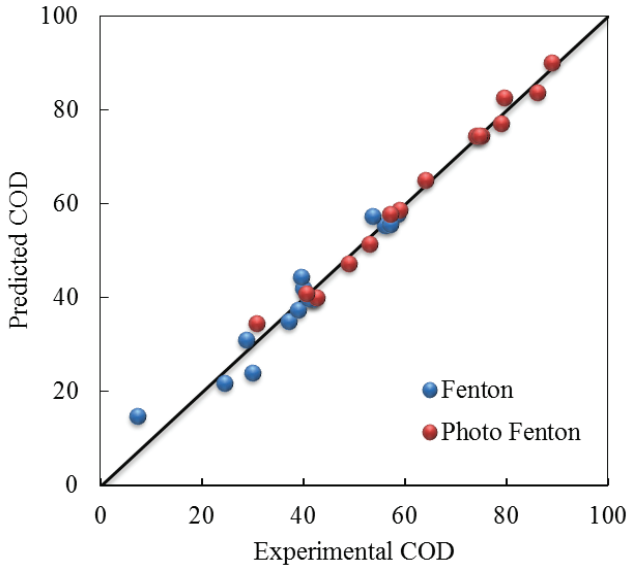

Fig. 5. Comparing the experimental and predicted values for the removal of COD in Fenton and photo-Fenton processes.

is explored along with degradation of pCNB. Furthermore, in this study the removal of COD in all runs and processes was examined at 30 min after reaction, but the degradation of pCNB was explored after 20 min, because in both processes the removal of COD was slower than pCNB, based on the probably formation of resistant intermediate products. Different initial concentration of pCNB had different COD, for example, about 200 mg/L of COD was exerted from 0.63 mM of pCNB. The remaining amounts of COD in various runs can be calculated by the initial amounts and the removal percentage of COD (Eq. (4)). The removal efficiency of COD in Fenton and photo-Fenton processes is presented in Figs. 6 and 7, respectively.

The removal of COD was enhanced by an increase in the dosage of ferrous ion from 0.08 to 0.14 mM and then reduced until 0.20 mM. Based on the experimental results, it is apparent that the effect of the ferrous ion concentration in Fenton process is higher than photo-Fenton ones. This can be related to the extensive regeneration of all Fe^{3+} to Fe^{2+} improved by UV [30]:

$$H_2O + Fe^{3+} + h\nu \rightarrow OH^{\bullet} + H^{+} + Fe^{2+} \quad (14)$$

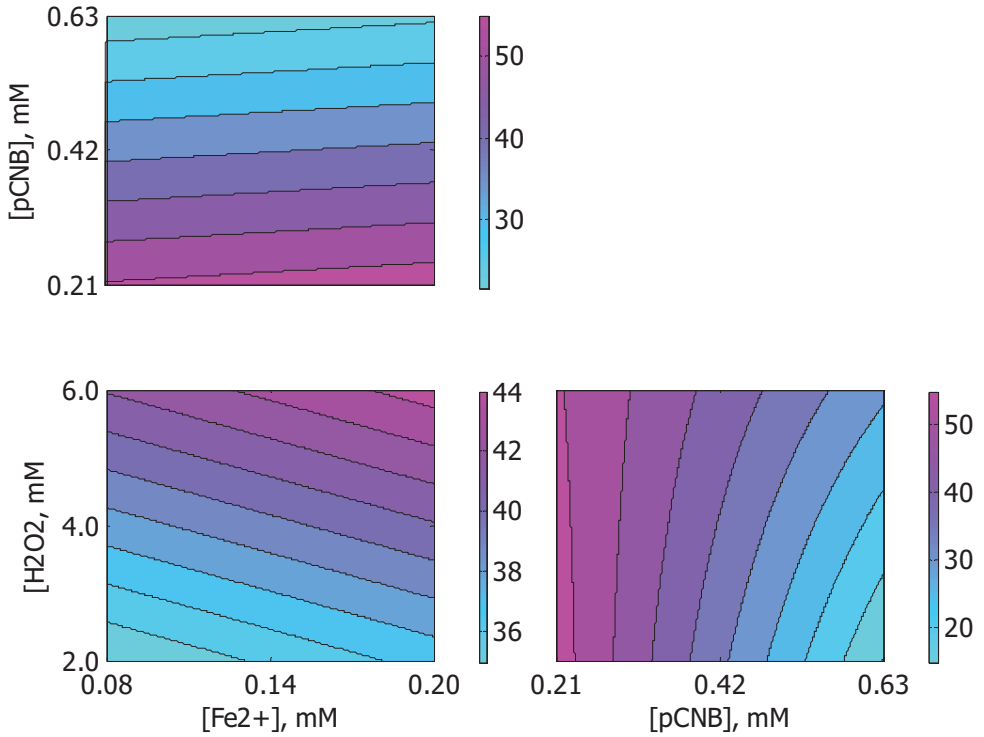

Fig. 6. The contour plot for the removal of COD in Fenton process based on [Fe^{2+}], [H_2O_2] and [pCNB].

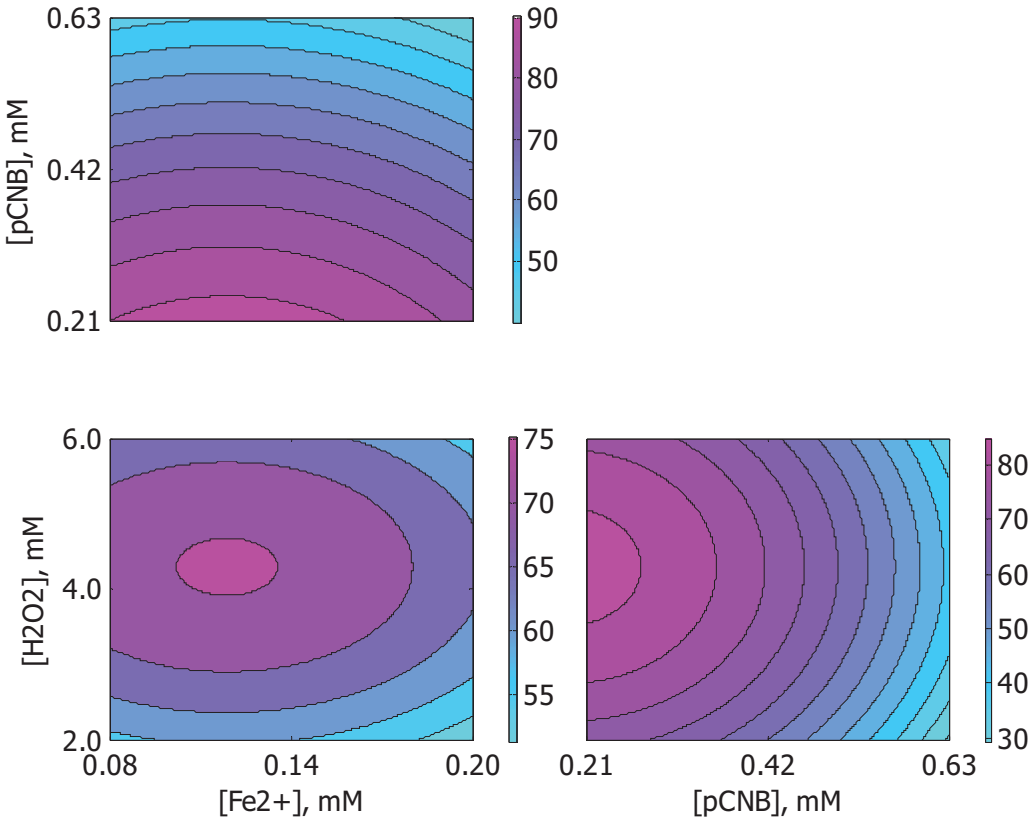

Fig. 7. The contour plot for the removal of COD in photo-Fenton process based on [Fe^{2+}], [H_2O_2] and [pCNB].

The Fenton process can degrade pCNB efficiently, but somewhat have difficulty with the removal of COD. The remaining ferrous ions were separated by changing the pH of the solution to the alkaline media, at the end of the processes [31].

The influence of the initial dosage of pCNB on the removal efficiency of pCNB and COD was explored and presented in Figs. 3 and 6 for Fenton process and in Figs. 4 and 7 for photo-Fenton process. It was obvious that the removal efficiency of pCNB and COD was decreased with improving the initial concentration of the pCNB from 0.21 to 0.63 mM, in Fenton and photo-Fenton processes.

The quantity of pCNB molecules was improved by an increase in the concentration of pollutant. Therefore, there was not enough hydroxyl radical and the removal efficiency of pCNB and COD decreased [32]. In photo-Fenton process, the diffusion of photons entering to the solution is reduced at high dosages of pollutant, so the generation of hydroxyl radical is decreased [33,34].

The contour plots for the removal of COD in Fenton and photo-Fenton processes are presented in Figs. 6 and 7, respectively.

4. Conclusions

In this study the BBD method and RSM were employed for the removal of pCNB, and COD in aqueous environment by Fenton and photo-Fenton processes.

The amounts of variables including, initial concentrations of H_2O_2, pollutant and Fe^{2+} were optimized for the removal of pCNB and COD. The ANOVA tests were performed to determine the significance of independent variables on the response function. The combined effect of variables on the responses has been inspected and a second-order polynomial model was fitted to the experimental data.

The use of UV light in Fenton process considerably decreases the amount of chemicals and time necessity. In optimum conditions, the removal of COD in photo-Fenton process was more effective (91.4%) than Fenton ones (58.5%) at 30 min of reaction. Also, after 20 min of remediation, the maximum values for the removal of pCNB in photo-Fenton and Fenton processes were 100% and 98.5%, respectively. The Fenton process can degrade pCNB efficiently, but somewhat has difficulty with the removal of COD.

The benefit of the photo-Fenton process was the low sludge creation, less chemicals, and time obligation but at the cost of power consumed. The power consumption can be reduced by using sunlight instead of artificial UV light to a larger amount.

Acknowledgment

The authors wish to thank the National Petrochemical Company of Iran for its scientific guidances.

References

[1] H. Bao, J. Gao, Y. Liu, Y. Su, A study of biodegradation/γ-irradiation on the degradation of p-chloronitrobenzene, Radiat. Phys. Chem., 78 (2009) 1137–1139.
[2] J. Shen, Z. Chen, Z. Xu, X. Li, B. Xu, F. Qi, Kinetics and mechanism of degradation of p-chloronitrobenzene in water by ozonation, J. Hazard. Mater., 152 (2008) 1325–1331.
[3] Y. Liu, J. Shen, Z. Chen, Y. Liu, Degradation of p-chloronitrobenzene in drinking water by manganese silicate catalyzed ozonation, Desalination, 279 (2011) 219–224.
[4] X.D. Zhu, Y.J. Wang, R.J. Sun, D.M. Zhou, Photocatalytic degradation of tetracycline in aqueous solution by nanosized TiO_2, Chemosphere, 92 (2013) 925–932.
[5] A. Shokri, K. Mahanpoor, D. Soodbar, Degradation of Ortho-Toluidine in petrochemical wastewater by ozonation, UV/O_3, O_3/H_2O_2 and UV/O_3/H_2O_2 processes, Desal. Wat. Treat., 57 (2016) 16473–16482.
[6] R.A. Palominos, M.A. Mondaca, A. Giraldo, G. Peñuela, M. Pérez-Moya, H.D. Mansilla, Photo catalytic oxidation of the antibiotic tetracycline on TiO_2 and ZnO suspensions, Catal. Today, 144 (2009) 100–105.
[7] P. Gharbani, A. Mehrizad, Heterogeneous catalytic ozonation process for removal of 4-chloro-2-nitrophenol from aqueous solutions, J. Saudi Chem. Soc., 18 (2014) 601–605.
[8] Q.N. Liao, F. Ji, J.C. Li, X. Zhan, Z.H. Hu, Decomposition and mineralization of sulfaquinoxaline sodium during UV/H_2O_2 oxidation processes, Chem. Eng. J., 284 (2016) 494–502.
[9] A.G. Trovó, S.A.S. Melo, R.F.P. Nogueira, Photo degradation of the pharmaceuticals amoxicillin, bezafibrate and paracetamol by the photo-Fenton process—application to sewage treatment plant effluent, J. Photochem. Photobiol., A, 198 (2008) 215–220.
[10] L.S. Leite, B.S. Maselli, G.A. Umbuzeiro, R.P. Nogueira, Monitoring ecotoxicity of disperse red 1 dye during photo-Fenton degradation, Chemosphere, 148 (2016) 511–517.
[11] A. Babuponnusami, K. Muthukumar, A review on Fenton and improvements to the Fenton process for wastewater treatment, J. Environ. Chem. Eng., 2 (2014) 557–572.
[12] P. Bautista, A.F. Mohedano, J.A. Casas, J.A. Zazo, J.J. Rodriguez, An overview of the application of Fenton oxidation to industrial wastewater treatment, J. Chem. Technol. Biotechnol., 83 (2008) 1323–1338.
[13] L. Clarizia, D. Russo, I. Di Somma, R. Marotta, R. Andreozzi, Homogeneous photo-Fenton processes at near neutral pH: a review, Appl. Catal., B, 209 (2017) 358–371.
[14] R.F.P. Nogueira, A.G. Trovo, M.R.A. da Silva, R.D. Villa, M.C. de Oliveira, Fundaments and environmental applications of Fenton and photo-Fenton processes, Quim. Nova, 30 (2007) 400–408.
[15] APHA-AWWA-WEF, Standard Methods for the Examination of Water and Wastewater, 20th ed., American Public Health Association, Washington, D.C., 1999.
[16] K. Elsousy, A. Hussen, K. Hartani, H.E. Aila, Elimination of organic pollutants using supported catalysts with hydrogen peroxide, Jordan J. Chem., 2 (2007) 97–103.
[17] S.L.C. Ferreira, R.E. Bruns, H.S. Ferreira, G.D. Matos, J.M. David, G.C. Brandao, E.P. da Silva, L.A. Portugal, P.S. Dos Reis, A.S. Souza, W.N.L. Dos Santos, Box-Behnken design: an alternative for the optimization of analytical methods, Anal. Chim. Acta, 597 (2007) 179–186.
[18] H. Moradi, S. Sharifnia, F. Rahimpour, Photo catalytic decolorization of reactive yellow 84 from aqueous solutions using ZnO nanoparticles supported on mineral LECA, Mater. Chem. Phys., 158 (2015) 38–44.
[19] A. Shokri, K. Mahanpoor, D. Soodbar, Evaluation of a modified TiO_2 (GO–B–TiO_2) photo catalyst for degradation of 4-nitrophenol in petrochemical wastewater by response surface methodology based on the central composite design, J. Environ. Chem. Eng., 4 (2016) 585–598.
[20] S. Giannakis, I. Hendaoui, S. Rtimi, J. Furbringer, C. Pulgarin, Modeling and treatment optimization of pharmaceutically active compounds by the photo-Fenton process: the case of the antidepressant Venlafaxine, J. Environ. Chem. Eng., 5 (2017) 818–828.
[21] A. Kumar, B. Prasad, I.M. Mishra, Optimization of process parameters for acrylonitrile removal by a low-cost adsorbent using Box–Behnken design, J. Hazard. Mater., 150 (2008) 174–182.
[22] E.C. Catalkaya, F. Sengul, Application of Box–Wilson experimental design method for the photo degradation of bakery's yeast industry with UV/H_2O_2 and UV/H_2O_2/Fe (II) process, J. Hazard. Mater., 128 (2005) 201–207.

[23] M.J. Lioua, M.C. Lub, J.N. Chena, Oxidation of explosives by Fenton and photo-Fenton processes, Water Res., 37 (2003) 3172–3179.
[24] I. Nitoi, T. Oncescu, P. Oancea, Mechanism and kinetic study for the degradation of lindane by photo-Fenton process, J. Ind. Eng. Chem., 19 (2013) 305–309.
[25] S.G. Schrank, H.J. Jose, R.F.P.M. Moreira, H.F. Schröder, Applicability of Fenton and H_2O_2/UV reactions in the treatment of tannery wastewaters, Chemosphere, 60 (2005) 644–655.
[26] P. Oancea, V. Meltzer, Photo-Fenton process for the degradation of Tartrazine (E102) in aqueous medium, J. Taiwan Inst. Chem. Eng., 44 (2013) 990–994.
[27] F. Abnisa, W.M.A. Wan Daud, J.N. Sahu, Optimization and characterization studies on bio-oil production from palm shell by pyrolysis using response surface methodology, Biomass Bioenergy, 35 (2011) 3604–3616.
[28] A. Shokri, Investigation of UV/H_2O_2 process for removal of Ortho-Toluidine from industrial wastewater by response surface methodology based on the central composite design, Desal. Wat. Treat., 58 (2017) 258–266.
[29] K. Keyvanloo, J. Towfighi, S.M. Sadrameli, A. Mohamadalizadeh, Investigating the effect of key factors, their interactions and optimization of naphtha steam cracking by statistical design of experiments, J. Anal. Appl. Pyrolysis, 87 (2010) 224–230.
[30] U. Bali, E.C. Catalkaya, F. Sengul, Photochemical degradation and mineralization of phenol: a comparative study, J. Environ. Sci. Health, Part A, 38 (2003) 2259–2275.
[31] X.K. Zhao, G.P. Yang, Y.J. Wang, X.C. Gao, Photochemical degradation of dimethyl phthalate by Fenton reagent, J. Photochem. Photobiol., A, 161 (2004) 215–220.
[32] J.H. Ramirez, F.M. Duarte, F.G. Martins, C.A. Costa, L.M. Madeira, Modelling of the synthetic dye Orange II degradation using Fenton's reagent: from batch to continuous reactor operation, Chem. Eng. J., 148 (2009) 394–404.
[33] N. Daneshvar, M. Rabbani, N. Modirshahla, M.A. Behnajady, Photo oxidative degradation of Acid Red 27 in a tubular continuous-flow photo reactor: influence of operational parameters and mineralization products, J. Hazard. Mater., 118 (2005) 155–160.
[34] G. Ginni, S. Adishkumar, J.R. Banu, N. Yogalakshmi, Treatment of pulp and paper mill wastewater by solar photo-Fenton process, Desal. Wat. Treat., 52 (2014) 2457–2464.